JOURNAL OF NANO- AND ELECTRONIC PHYSICS
Vol. 6 No 1, 01006(4pp) (2014)

ЖУРНАЛ НАНО- ТА ЕЛЕКТРОННОЇ ФІЗИКИ
Том 6 № 1, 01006(4cc) (2014)

Simulation Study on the Open-Circuit Voltage of Amorphous Silicon *p-i-n* Solar Cells Using AMPS-1D

B.M. Omer[1,2,*], F.A. Mohammed[3], A. Seed Ahmed Mahgoub[2,4]

[1] *Department of Physics, College of Science and Arts-Ranyah, Taif University, Ranyah - Kingdom Saudi Arabia*
[2] *Department of Applied Physics and Mathematics, Faculty of Applied Science and Computer, Omdurman Ahlia University, P.O. Box 786, Omdurman - Sudan*
[3] *Department of Mathematics and Physics, Faculty of Education, University of Kassala, Kassala - Sudan*
[4] *Department of Physics, Faculty of Education, University of Khartoum, P.O.Box 406, Khartoum - Sudan*

(Received 22 September 2013; published online 06 April 2014)

AMPS-1D (Analysis of Microelectronic and Photonic Structure) simulation program was used to simulate Amorphous Silicon p-i-n Solar Cell. The simulated result of illuminated current density-voltage characteristics was in a good agreement with experimental values. The dependence of the open-circuit voltage on the characteristics of the a-Si:H intrinsic layer was investigated. The simulation result shows that the open-circuit voltage does not depend on the thickness of the intrinsic layer. The open-circuit voltage decreases when the front contact barrier height is small or the energy gap of the intrinsic layer is small. The open-circuit voltage increases when the distribution of the tail states is sharp or the capture cross sections of these states are small.

Keywords: AMPS-1D, Modeling, Amorphous Silicon solar cell, Open-circuit voltage.

PACS numbers: 78.20.Bh, 73.40.Lq

1. INTRODUCTION

Carlson and Wronski reported the first Amorphous silicon solar cell in 1976 [1]. Amorphous silicon solar cells have been used in some portable electronic devices such as calculators and digital watches since the early 1980s. An efficiency of about 10 % was reported for *a*-Si : H *p-i-n* solar cells [2]. However, *a*-Si : H solar cells suffer from a light-induced degradation effect and stabilize only at low efficiency values [3]. One of the strategies to improve the efficiency of the solar cell is to improve the open-circuit voltage (V_{OC}). The open-circuit voltage of *p-i-n* solar cell is among its most important device parameters. The open-circuit voltage appears to be sensitive to many material and device parameters [4, 5]. Analytical and numerical modeling of the current density – voltage (J-V) characteristic of *a*-Si : H *p-i-n* have been presented in many works [6, 7]. In this paper, we present simulation results on the open-circuit voltage of amorphous silicon *p-i-n* solar cells. The computer calculations throughout this paper were done by using the AMPS-1D computer program from Pennsylvania State University [8]. The aim of this paper is to investigate the influence of the intrinsic layer characteristics on the open-circuit voltage of the *a*-Si : H *p-i-n* solar cell and to compare the results with both theoretical and experimental results found in the literature.

2. SIMULATION MODEL

Numerical modeling is a necessity for the realistic description of photovoltaic devices. By using simulation programs, it is possible to examine the influence of model parameters on device performance. Device modeling involves the numerical solution of a set of equations, which form a mathematical model for device operation, and the models that describe material properties and device operation processes. The usefulness of the simulation results strongly depends on the reliability of the input parameters that are required by the internal numerical models. AMPS-1D program is written by Professor Stephen Fonash and his group at the Pennsylvania State University. It is a very general program for analyzing and designing transport in microelectronic and photonic structures. The principal equations solved by AMPS-1D (using finite differences and Newton-Raphson technique) are:

$$\frac{d}{dx}\left(-\varepsilon(x)\frac{d\psi}{dx}\right)=\rho \tag{1}$$

$$\frac{1}{q}\left(\frac{dJ_n}{dx}\right)=-G_{op}(x)+R(x) \tag{2}$$

$$\frac{1}{q}\left(\frac{dJ_p}{dx}\right)=G_{op}(x)-R(x) \tag{3}$$

$$J_n(x)=q\mu_n n\left(\frac{dE_{fn}}{dx}\right) \tag{4}$$

$$J_p(x)=q\mu_p p\left(\frac{dE_{fp}}{dx}\right) \tag{5}$$

The first equation (1) is the Poisson equation where ρ is the space charge density and given by:

$$\rho=q.[p(x)-n(x)+N_D^+(x)-N_A^-(x)+p_t(x)-n_t(x)] \tag{6}$$

the electrostatic potential ψ and the free electron n, free hole p, trapped electron n_t, and trapped holes p_t, as well as the ionized donor-like doping N_D^+ and ionized accep-

* bushra_omer4@yahoo.com

tor-like doping N_A^- concentrations are all functions of the position coordinate x. Here, ε is the permittivity and q is the elementary charge. Equations (2) and (3) are the continuity equations for electrons and holes respectively. J_n and J_p are, respectively the electron and hole current densities. The term $R(x)$ is the net recombination rate resulting from band-to-band (direct) recombination and Shockley-Read-Hall (S-R-H) (indirect) recombination traffic through gap states. $G_{op}(x)$ is the optical generation rate as a function of x due to externally imposed illumination. In equations (4) and (5), μ_n and μ_p are the electron mobility and hole mobility, respectively. It is important to note that equations (4) and (5) are very general formulations that include diffusion, drift, and motion due to effective fields arising from band gap, electron affinity, and densities-of-states gradients. The model used in AMPS-1D for the net recombination term $R(x)$ in the continuity equations takes both direct recombination R_D and indirect recombination R_I processes into consideration such that:

$$R(x) = R_D(x) + R_I(x) \tag{7}$$

The net direct recombination rate is given by

$$R_D(x) = b_R\left(np - n_0 p_0\right) \tag{8}$$

Where b_R is the direct band-to-band recombination strength, n and p are the band carrier concentrations present when devices subjected to a voltage bias, light bias, or both. n_0(p_0) is the intrinsic electron (hole) density.

For S-R-H net recombination the trapping through each group of defects of density N_t is given by

$$R_I(x) = \frac{\left(np - n_0 p_0\right)}{\left(\tau_{p0}\left(n + n_t\right) + \tau_{n0}\left(p + p_t\right)\right)} \tag{9}$$

Where τ_{p0} and τ_{n0} are short hand for reciprocals of the thermal velocity-hole/electron capture cross section and N_t product. The quantities n_t and p_t depends exponentially on the position of the defects in the energy gap.
The optical generation rate $G_{op}(x)$ is expressed as:

$$G_{op}(x) = -\frac{d}{dx}\sum_i \varphi_i^{FOR}\left(\lambda_i, x\right) + \frac{d}{dx}\sum_i \varphi_i^{REV}\left(\lambda_i, x\right) \tag{10}$$

Where, ϕ_i^{FOR} and ϕ_i^{REV} are, respectively, the photon flux of the incident light and the light reflected from the back surface at a wavelength, λ of i at some point x, depending on the light absorption coefficient, and the light reflectance in the forward and reverse direction. The single junction a-Si : H solar cell in this work contains of three principle layers: a p-type a-SiC : H layer, an intrinsic a-Si : H layer and n-type a-Si : H layer, which form a p-i-n junction. The doped layers are very thin, the thickness of the p and n layers are 12 and 25 nm, respectively. The doped layers set up an internal electric field a cross the intrinsic a-Si : H layer. The intrinsic layer with an optical band gap of 1.73 eV serves as absorber layer. The electron-hole pairs generated in absorber layer experience the internal electric field, which facilitates separation of electrons and holes. The input parameters of the solar cell simulation was taken from the literature, however some parameters was changed slightly to have a very good agreement between the simulated J-V characteristics (under illumination) and the experimentally measured characteristics reported in reference [9]. The solar cell simulated with these parameters will be referred as the reference cell. When considering the sensitivity of open-circuit voltage to any given parameter, we will hold all other parameters constant and equal to their values given in table 1.

3. RESULTS AND DISCUSSION

At first, a verification of the solar cell device parameters was conducted through a careful reproduction of experimental J-V curve reported by Zeman in reference [9]. Figure 1 depicts the good matching of the simulated J-V to the experimental illuminated J-V characteristics of the solar cell. From the simulation the performance characteristics were: short circuit current density (J_{sc}) = 14.698 mA/cm^2, open circuit voltage (V_{OC}) = 0.834 V, fill factor (FF) = 0.655, and power conversion efficiency (η) = 8.023 %. The simulation results were in good agreement with the experimental short circuit current density (14.9 mA/cm^2), open circuit voltage (0.81 V), fill factor (0.66) and efficiency (8.0 %) found in the literature [9]. A reference input file corresponding to the matched parameters of this cell was then used as a baseline for further simulations. The open-circuit voltage was calculated for different set of input parameters.

Figure 2 shows the open-circuit voltage as a function of I-layer thickness for a different front contact barrier height. The open-circuit voltage depends strongly on the values of the front contact barriers height. The open-circuit voltage increased from 0.431 volt for barrier height of 0.95 eV to 0.834 volt for barrier height of 1.54 eV. The I-layer thickness varies between 300 nm to 450 nm, while the p-layer and the n-layer were fixed to 12 nm and 25 nm, respectively. In agreement with a previous results by Eric A. Schiff [11] the open-circuit voltage is nearly independent of the I-layer thickness.

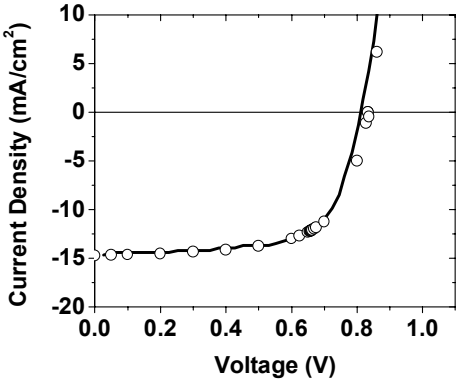

Fig. 1 – Illuminated current density-voltage plot of our simulation (line) compared with measured (open circles) from the work of Zeman [9]

Figure 3 shows the open-circuit voltage as a function of the band gap of the intrinsic absorber layer for different front contact potential barrier height. The relation corresponding to a barrier height (1.54 eV) is a straight-line relation with a slope of (0.991) which is slightly less

Table 1 – Layer and general device parameters

Parameter	Symbol	*P*	*I*	*N*
Relative permittivity,	EPS	11.90	11.90	11.90
Electron mobility (cm^2/Vs)	MUN	20 [4]	20 [4]	20 [4]
Hole mobility (cm^2/Vs)	MUP	4 [4]	4 [4]	4 [4]
Doping concentration of acceptors (cm^{-3})	NA	1.6×10^{19} [10]	0	0
Doping concentration of donors (cm^{-3})	ND	0	0	1×10^{19} [10]
Electrical band gap (eV)	EG	2 [4]	1.73 [9]	1.80 [4]
Effective density of states in the conduction band (cm^{-3})	NC	2×10^{20} [4]	2×10^{20}[4]	2×10^{20} [4]
Effective density of states in the valence band (cm^{-3})	NV	2×10^{20} [4]	2×10^{20}[4]	2×10^{20} [4]
Electron affinity (eV)	CHI	3.89 [4]	4 [4]	4 [4]
Thickness (nm)	L	12 [9]	300 [9]	25 [4]
The Gaussian donor state density (cm^{-3})	NDG	3×10^{18} [10]	5×10^{16}	9×10^{18} [4]
The donor Gaussian peak energy (eV)	EDONG	1.24	1.12	1.12
The standard deviation of the Gaussian donor level (eV)	WDSDG	0.15	0.15	0.15
Capture cross section of the donor like state for electrons (cm^2)	GSIG / ND	5×10^{-16} [4]	9×10^{-15}	1×10^{-14}
Capture cross section of the donor like state for holes (cm^2)	GSIG / PD	1×10^{-16} [4]	8×10^{-16}	1×10^{-15} [4]
The Gaussian acceptor state density (cm^{-3})	NAG	3×10^{18} [10]	5×10^{16}	9×10^{18} [4]
The acceptor Gaussian peak energy (eV)	EACPG	1.14	1.02	1.02
The standard deviation of the Gaussian acceptor level (eV)	WDSAG	0.15	0.15	0.15
Capture cross section of the acceptor like state for electrons (cm^2)	GSIG / NA	1×10^{-16} [4]	8×10^{-16}	1×10^{-15} [4]
Capture cross section of the acceptor like state for holes (cm^2)	GSIG / PA	5×10^{-16} [4]	9×10^{-15}	1×10^{-14}
Characteristic energy for donor-like tails (eV)	ED	0.12 [10]	0.05 [10]	0.05 [10]
Valence bandtail prefactor (cm^{-3}/eV)	GDO	4×10^{21} [10]	4×10^{21}[10]	4×10^{21} [10]
Capture cross section for electrons in donor tail states (cm^2)	TSIG / ND	1×10^{-16} [4]	5×10^{-16}[4]	1×10^{-15} [4]
Capture cross section for holes in donor tail states (cm^2)	TSIG / PD	1×10^{-17} [4]	1×10^{-16}[4]	1×10^{-17} [4]
Characteristic energy for acceptor-like tails (eV)	EA	0.07 [10]	0.03 [10]	0.03 [10]
Conduction bandtail prefactor (cm^{-3}/eV)	GAO	4×10^{21} [10]	4×10^{21} [10]	4×10^{21} [10]
Capture cross section for electrons in acceptor tail states (cm^2)	TSIG / NA	1×10^{-17} [4]	1×10^{-16} [4]	1×10^{-17}[4]
Capture cross section for holes in acceptor tail states (cm^2)	TSIG / PA	1×10^{-16} [4]	5×10^{-16} [4]	1×10^{-15} [4]

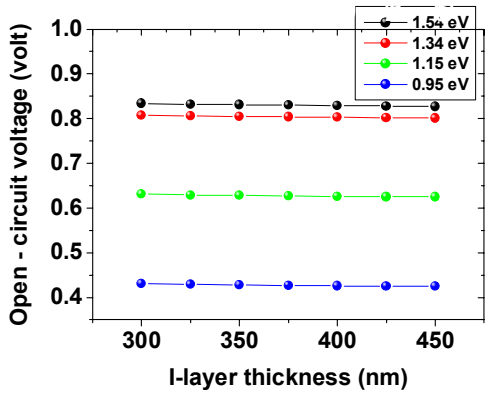

Fig. 2 – Open-circuit voltage versus I-layer thickness for a different front contact barrier height

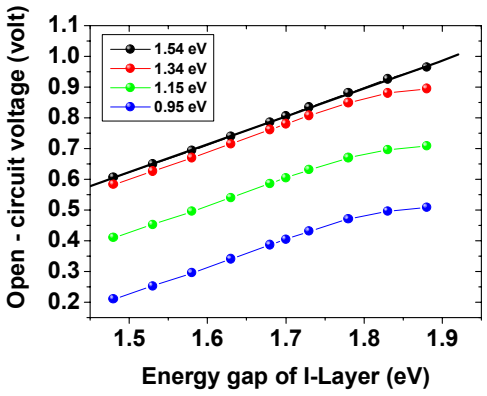

Fig. 3 – Open-circuit voltage as a function of optical band gap of the I-layer and a different contact barrier height, the black line is a linear fit

than unity. The relation shows that the cells deliver a voltage that is 0.745 volt below the band gap. This relation agrees well with the experimental relation [12]:

$$V_{OC} = \frac{E_g}{e} - 0.80 \qquad (10)$$

To analyze how the characteristic energy of the conduction band tail states (EA) affected the open-circuit voltage, we simulate the device varying the values of the characteristic energy in range between 0.03 eV and 0.07 eV. Figure 4 shows the relationship between the open-circuit voltage and the characteristic energy of the conduction band tail states. From figure 4 it is clear that the width of the conduction band tail could affect the open-circuit voltage significantly. The open-circuit voltage increase with the decrease of the characteristic energy of the conduction band tail states. Small values of EA and ED correspond to the sharp distribution of the tail states. The recombination rate of photo generated

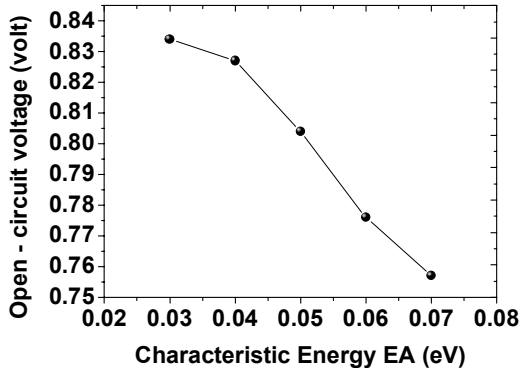

Fig. 4 – The open-circuit voltage versus the characteristic energy of the conduction band tail states (EA)

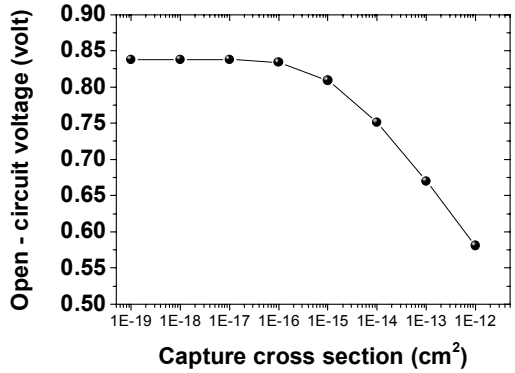

Fig. 5 – The open-circuit voltage versus capture cross section of the band tail states

carriers in the tail states decrease as shape of these states becomes sharp. A decrease of the conduction band tail characteristics energy from 0.07 eV to 0.03 eV causes a 77 mV increase in the open-circuit voltage.

Figure 5 shows the relation between the open-circuit voltage and the capture cross section of tail states. The open-circuit voltage increase with decreasing the capture cross section, the cell with the lower captures cross section will have a lower total recombination which resultsin a higher open-circuit voltage. Decreasing the capture cross section from 10^{-12} cm^2 to 10^{-16} cm^2 leads to 253 mV increase in the open-circuit voltage. The open-circuit voltage seems to saturate for the values of the capture cross section below 10^{-16} cm^2.

4. CONCLUSIONS

In conclusion, we simulated amorphous silicon *p-i-n* solar cell using AMPS-1D. We investigated the sensitivity of the open-circuit voltage on the characteristics of the *a*-Si : H intrinsic layer. The results show that the open-circuit voltage is nearly independent of the thickness of the intrinsic layer. The open-circuit voltage is governed by the intrinsic layer band gap. Our simulation suggested that for a sharp band tail states or small capture cross section the open-circuit voltage will increase.

AKNOWLEDGEMENTS

The authors are grateful to professor S. Fonash of the Pennsylvania State University for providing the AMPS-1D program used in the simulations.

REFERENCES

1. D.E. Carlson, C.R. Wronski, *Appl. Phys. Lett.* **28**, 671 (1976).
2. S. Benagli, D. Borrello, E. Vallat-Sauvain, J. Meier, U. Kroll, J. Hoetzel, J. Bailat, J. Steinhauser, M. Marmelo, G. Monteduro, L. Castens, *24th European Photovoltaic Solar Energy Conference*. (Hamburg: German: 2009).
3. D.L. Staeber, C.R. Wronski, *Appl. Phys. Lett.* **31**, 292 (1977).
4. U. Dutta, P. Chatterjee, *J. Appl. Phys.* **96**, 2261 (2004).
5. B. Yan, J. Yang, S. Guha, *Appl. Phys. Lett.* **83**, 782 (2003).
6. K. Misiakos, F.A. Lindholm, *J. Appl. Phys.* **64**, 383 (1988).
7. H. Tasaki, W.Y. Kim, M. Hallerdt, M. Konagai, K. Takahashi, *J. Appl. Phys.* **63**, 550 (1988).
8. Stephen J. Fonash, et al., *A manual for AMPS-1D for windows: A one-dimensional device simulation program for the analysis of microelectronic and photonic structures* (Pennsylvania State University: 1997).
9. B. Vet, Zeman, *Proceedings of the 9th STW Annual Workshop on Semiconductor Advances for Future Electronics and Sensors, 453* (Veldhoven: The Netherlands: STW: 2006).
10. A. Belfar, R. Mostefaoui, *J. Appl. Sci.* **11**, 2932 (2011).
11. Eric A. Schiff, *Sol. Energ. Mat. Sol. C* **78**, 567 (2003).
12. A. Luque, S. Hegedus, *Handbook of Photovoltaic Science and Engineering* (John Wiley & Sons: 2003).